

NUMERICAL SIMULATION OF SPOT WELDED STEEL SHEETS

Bianzeubé TIKRI^{1*}, Nadjitonon NGARMAIM², Djonglibet WEL-DORET¹,
Ngargueudedjim KIMTANGAR², Djimako BONGO², Jean-Louis ROBERT³

¹ University Polytechnic of Mongo (Chad)

² University of N'Djamena, Department of Technology

³ Institute Pascal, the University Blaise Pascal of Clermont-Ferrand (France)
Author for correspondence: Email: bitikri@gmail.com, tel.: (+235) 66 28 24 71

ABSTRACT

The welding process leads to heating of the very heterogeneous metal, volumes of material knowing the melting temperature levels. The subsequent cooling is heterogeneous from the point of view of the rate of change in temperature. The melted zone solidifies to reach the ambient temperature by changing the microstructure of the metal, the residual stresses and deformations. These are generated both by the heterogeneous nature of the temperature variations, by the crystal transformations related to the heat treatment induced by the welding and to the forces related to the lateral pressure imposed by the electrodes through which circulates the current required for the welding. This article aims to calculate the levels of stress encountered locally to justify the sites of initiation of fatigue cracks under tensile-shear load of specimens welded by point. Stress levels do not alone justify the fatigue behavior of a material when it does not exhibit homogeneous properties of fatigue resistance in the volume studied. Nevertheless, the distribution and stress levels encountered are a valuable contribution to the understanding of local fatigue damage, the sensitivity of stress levels and their spatial distribution in the welded spot and their immediate vicinity will be studied in relation to several geometric parameters which are variable in specimens. The aim of the numerical model implemented is therefore, to some extent, to identify the critical zones of the welded point and to quantify the influence of certain geometric hazards.

Keywords - Mesh optimization, constraints, ruin modes, welded point shear, sheet metal cracking

1. INTRODUCTION

The particular geometry of a welded point assembling two sheets generates high concentrations of stresses in the vicinity and even inside the welded point. These stresses cause the cracking and propagation of cracks under cyclic loading until one of the sheets or the molten core breaks. The cracking of the sheets and the shearing of the point are the two modes of fatigue damage of the assemblies made by welded points. In order to better understand the fatigue damage of the spot-welded specimens, the simulation of the welding process and the calculation of the stresses in the structure give a very valuable support to the analysis of the different modes of ruin of the specimens subjected to traction loads Time-varying shear. The objective of this article is to analyze

and to attempt to justify numerically the finite element method of the two observed modes of rupture of the specimens welded by point and stressed in tension-shear. The diameter of the welded point, the interface between the two sheets and the shape of the notch are the geometric parameters of this study. The calculation of the constraints was carried out by means of the calculation code by finite elements FEMAP-NASTRAN. This first paragraph is intended to present the geometric model used for the finite element calculations of the stresses existing in the test specimen subjected to tensile stress.

2. NUMERICAL MODEL OF THE WELDED SPECIMEN

2.1. Geometric model

The geometric model used is that shown in figure1. The test piece consists of two thin sheets of dimensions 124×30 mm (in mm) with a covering length of 38 mm. Two rectangular wedges of dimensions 38×30 (in mm) are used to locate the resultant of the tensile-shear stress in the plane of contact of the sheets. The two sheets and the two blocks are connected by the welded point produced by the resistance welding process. A three-dimensional analysis of the specimen was performed by finite elements to determine the distribution of normal and shear stresses within the welded spot. The objective is to try to correlate the two modes of fatigue ruin usually observed on the plates assembled by a welded point with the values of the stresses generated by the tensile-shear stress. One of the two mechanisms of fatigue is the cracking of the sheets, first in the thickness then by transverse propagation; the other is the transverse shear of the molten core of the welded point. The orthonormal reference (1, 2, 3) used for the whole study is shown in Fig.1. Due to the plane of symmetry (2, 3) of the test piece and its loading, only one half-test piece is modeled. This reduces calculation time. The loading is applied to the upper side of the specimen, the lower side being fixed (figure1a). The precision and the calculation times are highly dependent on the quality of the mesh of the welded point itself in the vicinity of the notch bottom. Finally, the EF model comprises 492,192 elements of isoperimetric type with 701,993 nodes (figure1b). The FEMAP-NASTRAN software is used to perform these calculations. The mechanical properties of elasticity of the steel used are a Young's modulus of $210,000 \text{ MPa}$ and a Poisson's coefficient of 0.3.

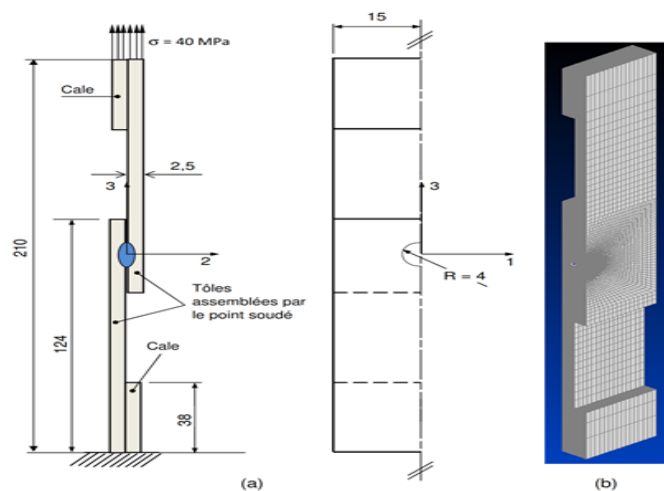


Figure 1 Geometrical model of the test piece "welded point" (a) drawing of definition, (b) mesh

The specimen is subjected to a tensile-shear stress in the form of a uniform tensile stress of 40 MP_a applied to the upper section of the test piece (figure. 1a). This type of stress corresponds to a tensile force of the test piece equal to 6000 N. In a first stage, the calculations are carried out within the framework of a purely elastic behavior of the material. In reality, the acuteness of the notch bottom and the elastoplastic behavior of the material generate local plasticity. The rupture of the test piece is linked to the predominance of one of the two modes of rupture in competition. The welding conditions and stress levels may be more favorable to one than to the other, which would then explain why one of the two leads to rupture before the other. The fig. 2 shows two similar test pieces, broken one by cracking one of the two sheets, the other by shearing the welded point.

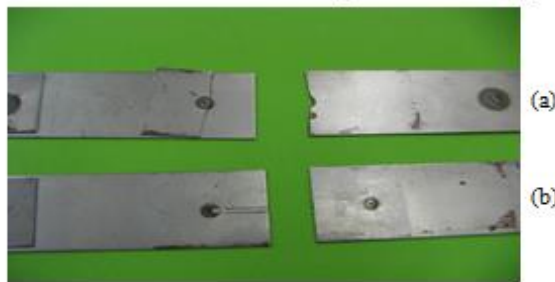


Figure 2 Specimens welded by spot and broken in two distinct modes of rupture (a) by cracking one of the two sheets, (b) by shearing the core of the welded point

2.2. Choice and optimization of the specimen mesh

Given the geometry of the specimen used, the study was based on three-dimensional modeling and therefore required voluminal elements.

The mesh size of the test piece adopted is that shown in Fig.1b. The model has 16 elements on half width (15 mm) and 34 elements in thickness (2.5 mm). In the fillet of the molten core with the two sheets, stress concentration zone, a fine mesh has been chosen for a better accuracy of the results (Fig.3).

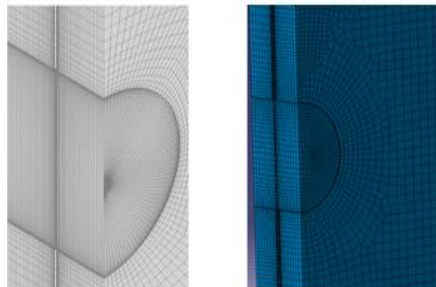


Figure 3 Mesh models used to optimize results

The preliminary study of the convergence of the mesh required the successive use of several element sizes. The final mesh retained is such that the size of the elements no longer influences the results obtained in terms of

constraints. Two particular zones are retained for the comparison of the results of calculations of the states of constraints obtained for each type of mesh. These zones contain the ignition sites of the two modes of fatigue failure of the welded points and are defined in Fig.4. Both are located in the plane of symmetry (2, 3) of the test piece. The first zone is the segment AB located on the internal face of one of the two assembled sheets; the point A belongs to the upper sheet and is therefore located on the side where the tensile force is applied. The second zone is the vertical diameter CD of the molten core with center O.

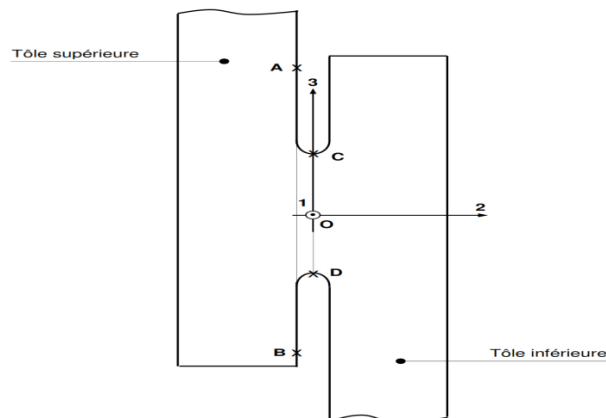


Figure 4 Local geometrical model at the welded point: description of the zones of comparison of the constraints for the optimization of the mesh in the plane of symmetry of the test piece.

The Figure 5 shows the evolution of the normal stress σ_{33} along the vertical diameter CD of the welded point of the test piece for four different meshes used: the mean mesh width in the fillet is 0.0754 mm (296,588 elements) In the first case, 0.0546 mm (368,524 elements) in the second, 0.0336 mm (492,192 elements) in the third and 0, 0294 mm (524,064 elements) in the latter case.

On all the stress distribution graphs on CD or on AB, one denotes the parameter which corresponds to the opposite of the dimension z in the overall reference of the test piece. The points A, B, C and D therefore have respectively abscissa -15, +15, - 4 and + 4 in FIGS. 5 and 7.

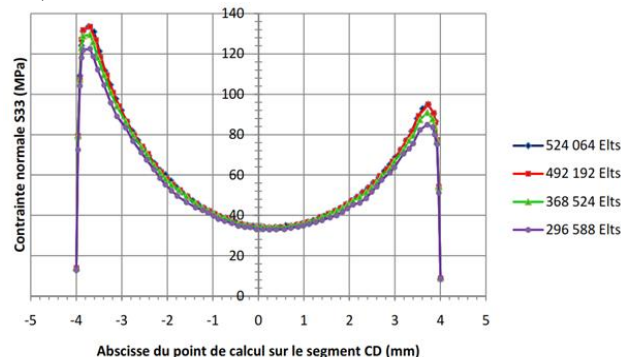


Figure 5 Comparison of the results of calculation of σ_{33} for the four mesh sizes analyzed

It is noted from Figure 5 that the evolutions of the normal stress σ_{33} for mesh sizes of 492,192 and 524,064 elements are confused.

For the sake of clarity, the result of the calculations is shown in Figure 6 for the last two mesh sizes. The two curves together show the convergence of stress calculations. The mesh with 492,192 elements was therefore retained for the following finite element calculations.

The Figure 7 shows the same comparison of the evolution of the normal stress σ_{33} for the last two meshes studied.

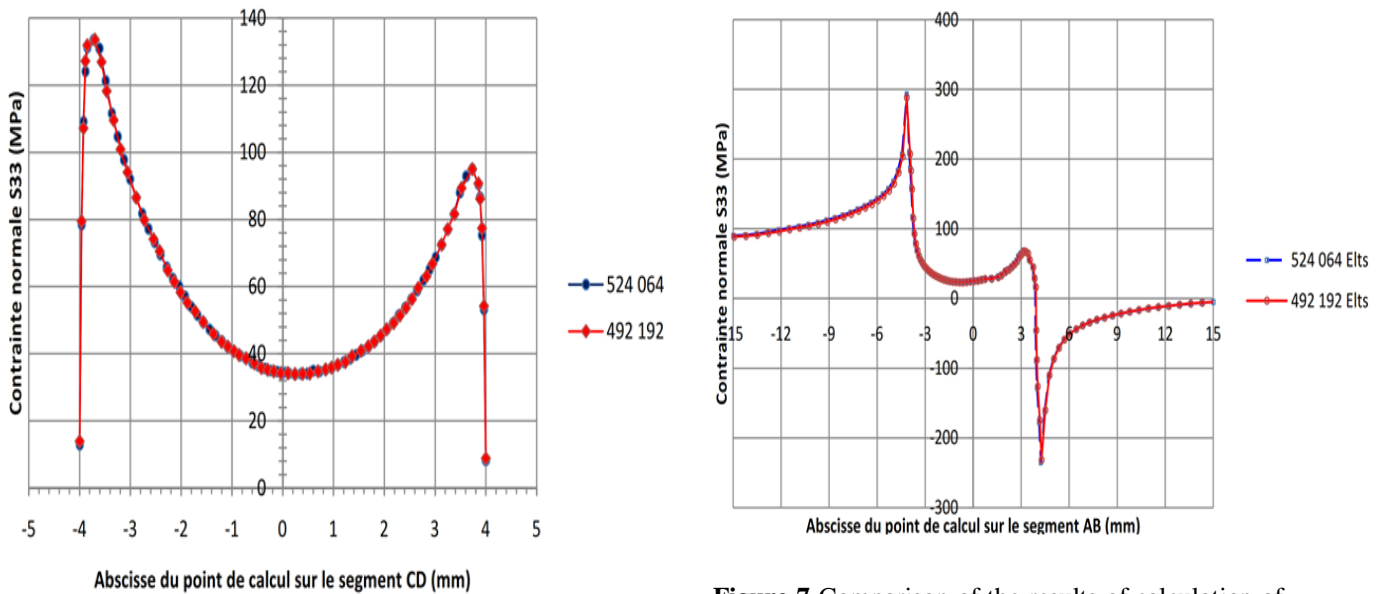


Figure 6 Comparison of the calculation results of CD σ_{33} for meshes with 492 192 and 524 064 elements

Figure 7 Comparison of the results of calculation of σ_{33} on the segment AB for the two meshes comprising 492 192 and 524 064 elements

The evolutions of the normal stress σ_{33} on AB for each of the last two meshes are also analogous and thus indicate the convergence of the results of calculation, which justifies here also to retain the mesh at 492 192 elements according to the principle retained.

3. STRESS ANALYSIS IN THE CASE OF ELASTIC BEHAVIOR

Local variations in the geometry of a structure, subjected to monotonic or cyclic loading, can lead to local amplification of the stress field with respect to its nominal value. Any sudden variation in cross section (notch, groove, hole, roundness, crack, etc.) locally amplifies the stresses, which generally leads to a significant weakening of the structure in terms of safety. In a test tube composed of two thin sheets assembled by a welded

point and subjected to uniaxial tension, the lines of force are concentrated at the level of the fillet connecting the molten core to the two sheets, greatly increasing the intensity of the local stresses. This principle of stress concentration greatly affects the fatigue strength in the case of variable loads. The analysis of the stress distribution in the area where the stress concentration is high, ie in the welded spot and its immediate vicinity, is therefore crucial for identifying sites of fatigue crack initiation and their criticality by comparing the stress levels.

3.1. Constraint Concentration Areas

The figure 8 shows (a) the shape of the deformed specimen under the tensile stress of 6000 N, (b) the distribution of the normal stress σ_{33} in the plane of symmetry of the welded spot, (c) The distribution of the tangential stress σ_{23} , always in the plane of symmetry of the welded point.

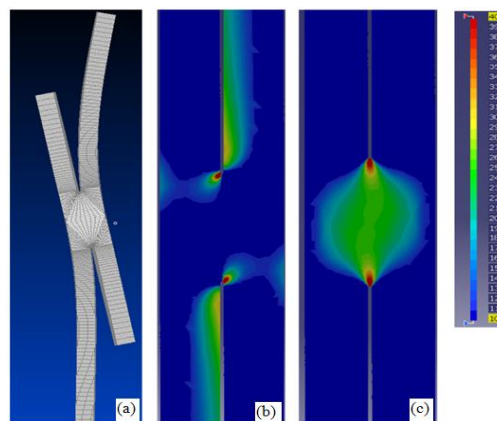


Figure 8 Analysis of the behavior of the "welded-point" specimen under tensile-shear stress (a) deformation of the plates, (b) distribution of the normal stress σ_{33} , (c) shear stress distribution σ_{23}

The two segments AB and CD thus appear well justified as places of study and comparison of the representative stresses existing within the points welded under a load of traction-shearing, since they contain the sites where the constraints are maximum. These sites are, in the case of a corrugated loading, those where the amplitude of the stresses is maximum; they are therefore critical areas from the point of view of fatigue.

3.2. Analysis of the influence of geometrical parameters on the distribution of stresses in the welded point

The observations of the fillet of the molten core on the sheets show a very variable shape of the notch bottom and of the interface between the sheets, even when all the test pieces examined are carried out with a protocol and similar welding conditions [4]. Moreover, as Radaj and Sonsino [3] point out, the shape of the notch floor varies according to the welding conditions and is not uniform or identical over the entire periphery of the point. This variation in the geometry of the specimen in the area of the welded spot probably plays a considerable role in the dispersion of the lifetimes of the test pieces under identical conditions. In order to understand this phenomenon and to try to explain the two modes of ruin observed, we propose to analyze the influence of the parameters likely to play a role in the mechanical behavior of the test piece. These parameters are the diameter

D of the core, the distance d between the plates (or interface) and the radius R of the fillet of the molten core on the two sheets. In figure 9 these three parameters are mentioned.

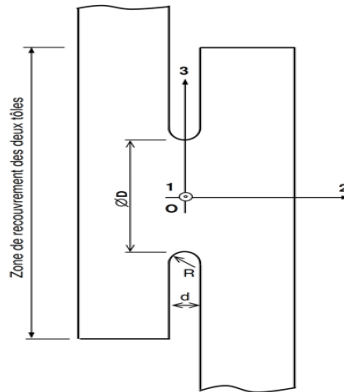


Figure 9: Definition of the geometric parameters of the test specimen

The parametric study is described and carried out within this paragraph. All the calculations carried out in this framework are assumed to be elastic. In order to facilitate the comparison base, the specimens are stressed in each case in tensile shear force by an effort of 6000 N.

3.2.1. Distribution and triaxiality of the stresses within the welded point on the segment AB and the diameter CD

The nature and the distribution of the stresses along the two comparison segments are established in a first time and presented in figs. 10 and 11. The parametric study itself will be discussed below. The fig. 10 shows the evolution of each of the 6 components of the stress tensor on the segment AB of the upper sheet. The fig. 11 gives the same evolution on the diameter CD, always for the same loading of the test piece (traction of 6000 N).

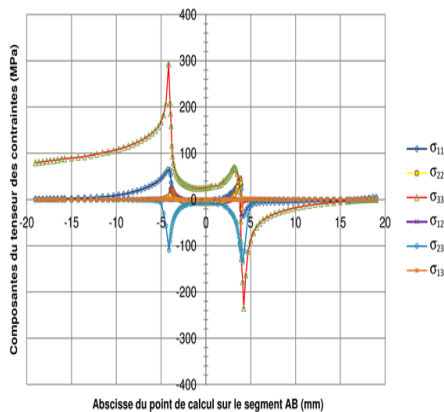


Figure10.1 Representation of the 6 components of the stress tensor on AB welded point

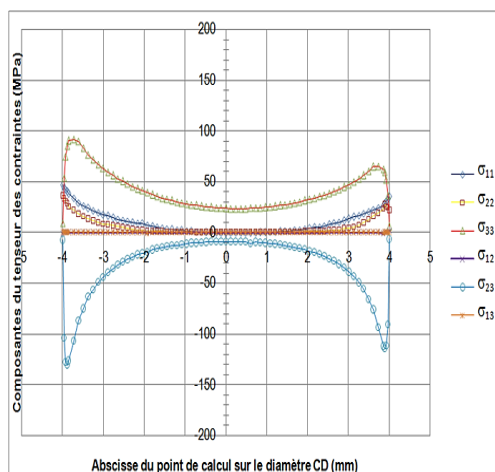


Figure 10.2 Representation of the 6 components of the stress tensor on the diameter CD of the welded point

At the level of the notch bottom to which the periphery of the molten core is related, a predictable stress peak appears very clearly in the two preceding figures because it is related to the concentration of stresses generated by the local geometry and the nature of the loading of the specimen.

It also appears that the components of constraints σ_{33} and σ_{23} are predominant. They are therefore the components of the most influential constraints on the mechanical strength of the welded point and will therefore be the main object of our numerical study.

The variability of the notch bottom and the interface between the sheets according to the test pieces can probably play a major role which explains the dispersion of the results of the lifetimes of the test specimens tested. In order to understand their effect on the two modes of fatigue failure of the material, a sensitivity analysis of the parameters likely to play a role in the mechanical behavior of the test piece is now discussed. This is the diameter D of the core, the distance d between the sheets and the radius R of the notch bottom (Figure 9). The analysis will consist in varying these parameters and analyzing their influence on the distribution of stresses on the two segments AB and CD.

3.2.2. Influence of diameter D of the welded-point nucleus

The test is carried out on specimens having a welded-point core with a diameter D equal to 5 mm, 8 mm or 10 mm respectively. The other two parameters, the interface between the two sheets and the shape of the notch (radius of the fillet), are kept constant at 0.15 mm and 0.075 mm respectively. The graphs of figures 11 and 12 relate the distribution of the normal and shear stresses as a function of the diameter of the core of the welded point.

a. Contraintes sur le diamètre CD du noyau fondu

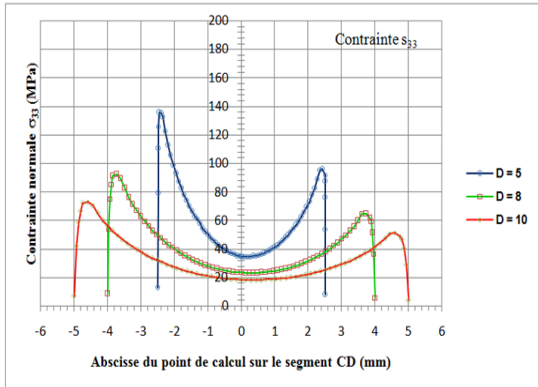


Figure 11.1 Distribution of the normal stress σ_{33} on the diameter CD for three different values of the diameter of the welded point

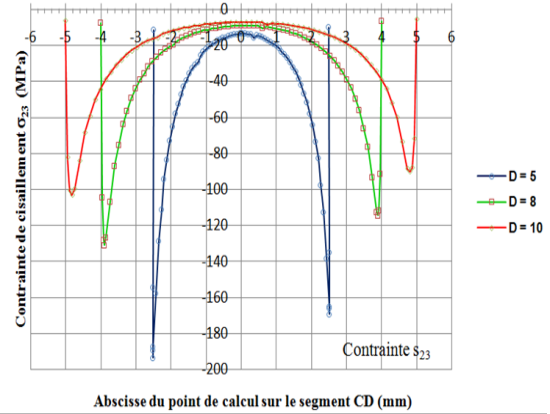


Figure 11.2 Distribution and shear stress σ_{23} on the CD diameter for three distinct values of the diameter of the welded point

b) Constraints on the segment AB (internal face of the sheet)

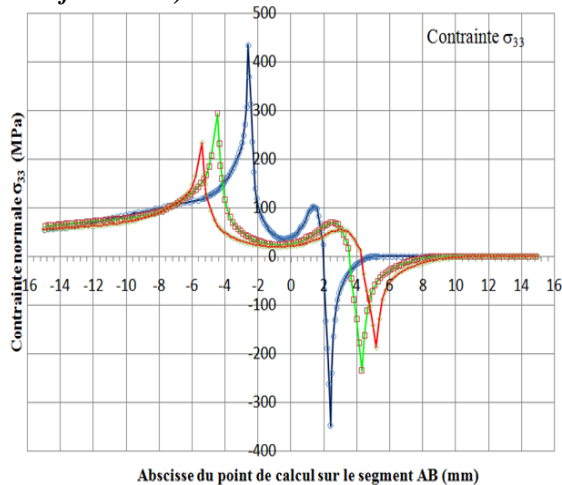


Figure 12.1 Distribution of the normal stress σ_{33} on the segment AB for three distinct values of the diameter of the welded point

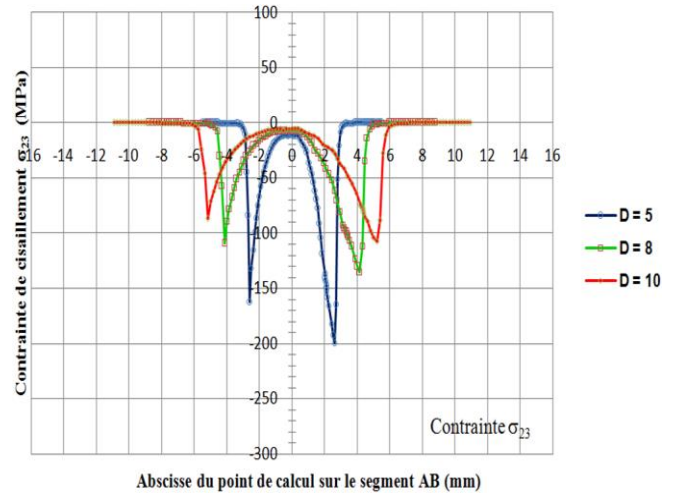


Figure 12.1 Distribution of the shear stress σ_{23} on the segment AB for three distinct values of the diameter of the welded point

The maximum values on the diameter CD and the segment AB of the normal stresses σ_{33} and shear stresses σ_{23} are summarized in Table 1. Figures 16 and 17 give a graphical representation on CD and AB respectively.

Table 1 Values of $\sigma_{23 \max}$ and $\sigma_{33 \max}$ on the diameter CD and the segment AB as a function of the diameter of the welded point for an applied stress-shearing force equal to 6000 N

	Diameter (mm)	$\sigma_{23 \max}$	$\sigma_{33 \max}$
Diameter CD	5	193	136
	8	131	93
	10	103	73
Segment AB	5	161	433
	8	109	293
	10	87	233

This first parametric study reveals the increase of the stresses σ_{33} and σ_{23} when the diameter of the core decreases, which seems quite logical with constant tensile force. Two other important lessons can be drawn from this study:

The tangential stress σ_{23} is preponderant in front of the normal stress σ_{33} on the diameter CD of the welded-point nucleus, which justifies the shear rupture of the molten core when this mode of ruin is observed. The ratio between $\sigma_{23 \max}$ and $\sigma_{33 \max}$ is about 1.4.

- On the segment AB, located on the internal face of the sheet, it is the normal stress σ_{33} which clearly takes precedence over the tangential stress σ_{23} (ratio of the order of 2.7 between $\sigma_{33 \max}$ and $\sigma_{23 \max}$). The rupture by cracking of the sheet is therefore justified on AB when the fatigue ruin occurs in this place. The cracking mechanisms are therefore not the same on the diameter CD and on the segment AB. There is competition between these two modes of ruin, one on the diameter CD in shear, the other in cracking on the internal face of the sheet. The respective crack propagation velocities lead one or the other of the two modes of ruin to win in the end. As such, it should be pointed out that a crack within one or both of the two sheets assembled by the welded point has always been observed in the case of shear rupture of the point. The inverse is more delicate to observe (beginning of cracking by shear of the molten core after rupture by cracking of one of the two plates) but it was in the framework of the work of thesis of F. Rossillon [4].

3.2.3. Influence of the interface between the two sheets

The figure13 shows the evolution of the normal and shear stresses as a function of the interface between the sheets. The diameter of the molten core is taken equal to 8 mm for this study; the shape of the notch bottom is circular with a radius equal to half the interface. The test is carried out on spot welded specimens with an interface between the two plates taken equal to 0.10 mm, 0.15 mm and 0.20 mm respectively. The calculation results, in terms of stresses σ_{33} and σ_{23} , are plotted on the diameter CD and the segment AB.

a) Constraints on the CD diameter of the molten core

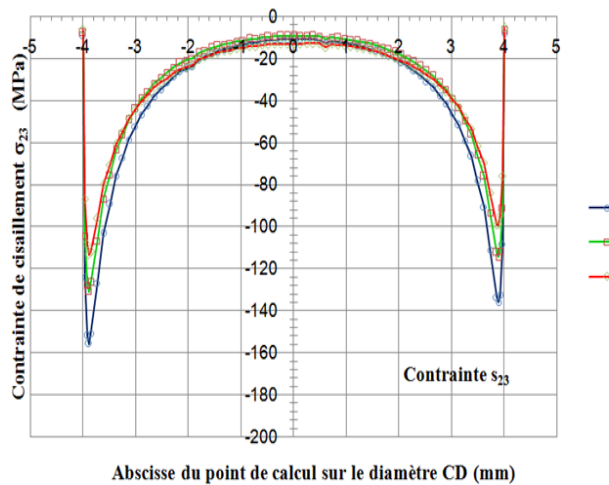


Figure 13.1 Distribution on the diameter CD of the normal stress σ_{33} for the three distinct values of the interface between plates

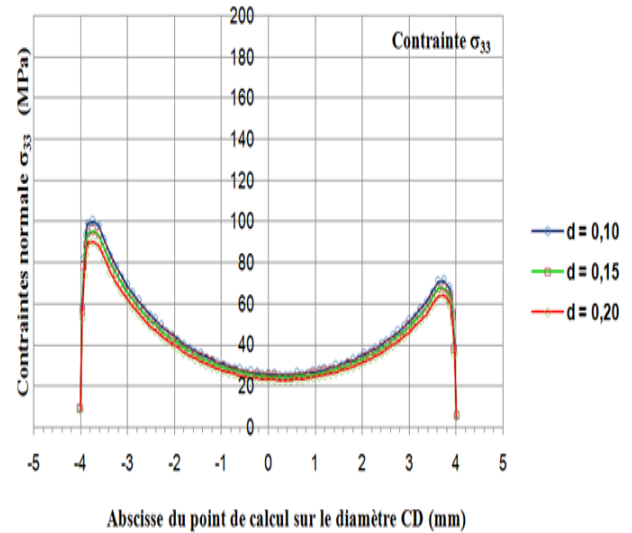


Figure 13.2 Distribution on the CD diameter of the shear stress σ_{23} for the three distinct values of the interface between sheets

b) Constraints on the segment AB (internal face of the sheet)

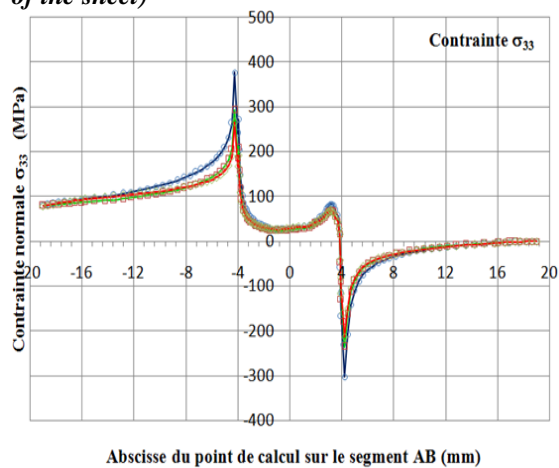


Figure 14.1 Distribution on the segment AB of the normal stress σ_{33} for the three distinct values of the interface between plates

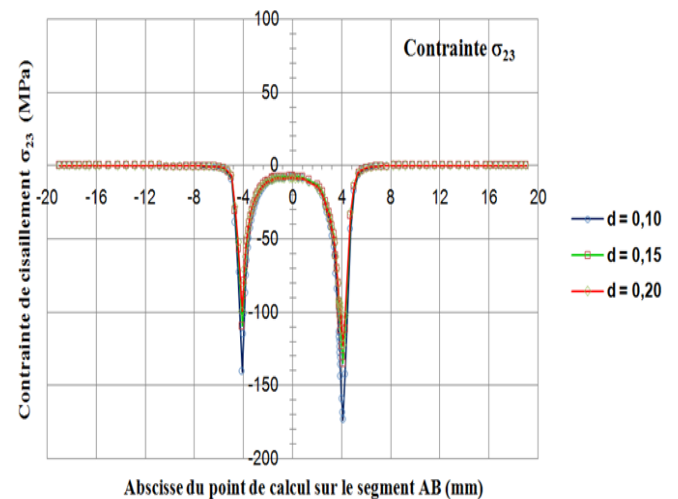


Figure 14.2 Distribution on the segment AB of the shear stress σ_{23} for the three distinct values of the interface between plates

The maximum values on the diameter CD and the segment AB of the normal stresses σ_{33} and shear stresses σ_{23} are summarized in Table 2 and are then plotted as a function of the value of the interface in Figures. CD and AB respectively).

Table 2 Values of $\sigma_{23 \max}$ and $\sigma_{33 \max}$ on the diameter CD and the segment AB as a function of the interface between the two sheet σ_{23} s for an applied tension-shear force equal to 6000 N

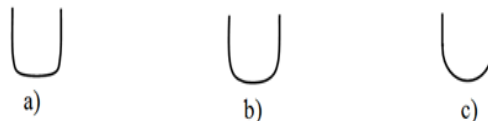
	Interface (mm)	$\sigma_{23 \max}$	$\sigma_{33 \max}$
Diameter CD	0.20	113	88
	0.15	131	94
	0.10	156	99
Segment AB	0.20	108	266
	0.15	134	293
	0.10	177	379

The first observation that emerges from this table is that the stress level increases when the interface between plates decreases. The increase in stress, when passing from an interface of 0.2 to 0.1 mm, is more marked for the maximum shear than for the maximum normal stress: ratios for $\sigma_{23 \max}$ of 1.38 and 1.63 On CD and AB respectively against ratios of 1.13 and 1.42 for $\sigma_{33 \max}$ on CD and AB.

The tangential stress is always preponderant over the normal stress on the diameter CD, and this preponderance is accentuated when the interface decreases. The tendency is inverse on the segment AB: the normal stress is preponderant in front of the tangential stress but the ratio $\sigma_{33 \max} / \sigma_{23 \max}$ decreases when the interface also decreases: it is 2.46 for $d = 0.20$ mm and increases to 2, When $d = 0.10$ mm.

3.2.4. Influence of the shape of the notch

The study is carried out on spot welded specimens, the fillet of the notch having a radius R equal to 0.025 mm, 0.05 mm and 0.075 mm respectively (figure 20 briefly describes the profile of the corresponding notch base to these three cases). The diameter of the molten core and the distance between the two sheets (interface) are equal to 8 mm and 0.15 mm respectively for this parametric study.



Figures 15 Different shapes studied from the notch bottom, as a function of the radius R of the fillet: a) R = 0.025 mm, b) R = 0.050 mm, c) R = 0.075 mm

The figures 16 to 17 show the distributions of the normal stresses σ_{33} and shear stresses σ_{23} as obtained by calculation on CD and AB, as a function of the radius of the fillet of the notch.

a) Constraints on the CD diameter of the molten core

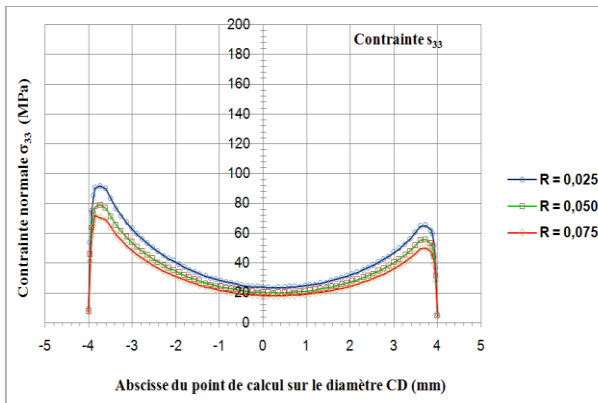


Figure16.1 Distribution on the CD diameter of the normal stress σ_{33} for the three different values of the radius of the fillet in the bottom of the notch

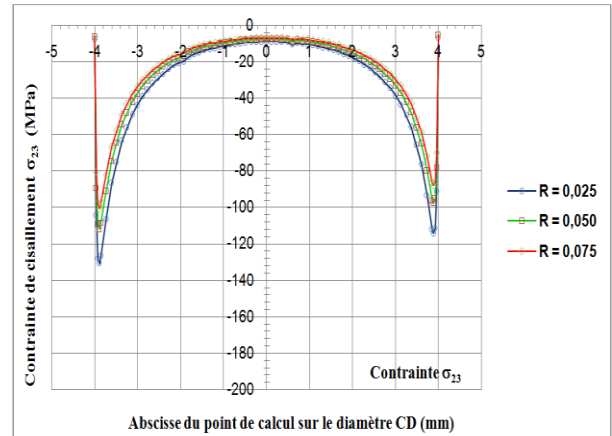


Figure16.2 Distribution on the CD diameter of the shear stress σ_{23} for the three different values of the radius of the fillet in the bottom of the notch

b) Constraints on the segment AB (internal face of the sheet)

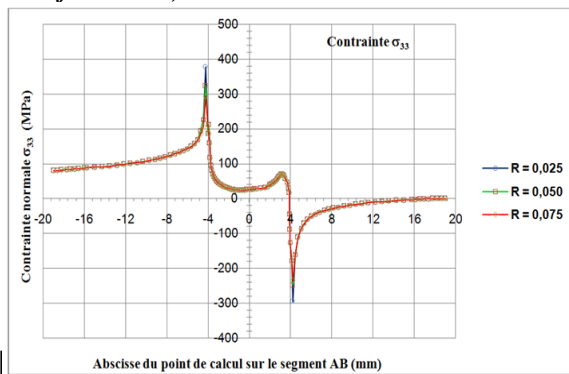


Figure17.1 Distribution on the segment AB of the normal stress σ_{33} for the three distinct values of the radius of the fillet at the bottom of the notch

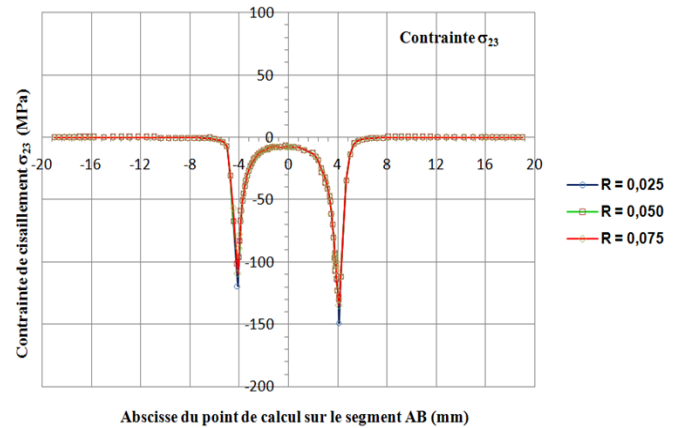


Figure17.2 Distribution the shear stress σ_{23} for the three distinct values of the radius of the fillet at the bottom of the notch

The maximum values on the CD diameter and AB segment of the normal stress σ_{33} and the shear stress σ_{23} are summarized in Table 3 below. FIGS. 29 and 30 give a graphical representation of these maximum stress values as a function of the radius of the fillet.

Table 3 Variation of $\sigma_{23 \text{ max}}$ and $\sigma_{33 \text{ max}}$ on the diameter CD and the segment AB as a function of the radius of the fillet at the bottom of the notch between the sheets

	Interface (mm)	$\sigma_{23 \text{ max}}$	$\sigma_{33 \text{ max}}$
Diameter CD	0.025	131	93
	0.050	112	80
	0.075	101	72
Segment AB	0.025	149	377
	0.050	119	324
	0.075	101	293

A particular point is to be noted as to the influence of the value of the radius of the fillet on the stress levels obtained. On the diameter CD, an increase in the radius leads to a decrease of the normal stress and of the shear stress. The same evolution is observed on the segment AB: the normal and maximum shear stresses decrease when the radius of the fillet increases. These results are logical because the acuity of the stress concentration in an angle or a shoulder decreases as the radius of the fillet increases.

The tangential stress σ_{23} is preponderant, over the diameter CD, in front of the normal stress σ_{33} , as was also observed in the previous parametric studies. On the AB segment, the preponderance order is reversed. It even increases when the radius of the fillet increases. Indeed, one passes from a ratio $\sigma_{33 \text{ max}} / \sigma_{23 \text{ max}}$ equal to 2.53 for $R = 0.025$ mm at a ratio equal to 2.90 for $R = 0.075$ mm. On the diameter CD, the ratio $\sigma_{23 \text{ max}} / \sigma_{33 \text{ max}}$ is independent of the value of the radius of the fillet.

3.3. Justification of experimental sites for crack initiation by the calculation of stresses

The calculation of the finite element stresses carried out during this work revealed the very clear predominance of the normal stress σ_{33} in front of the tangential component σ_{23} on the segment AB of the internal face of the spot welded specimen. FIG. 18, on the left, shows schematically the distribution of these normal and tangential stresses on the segment AB. The stress peak observed on the distribution of each of the two components lies at the foot of the fillet of the molten core on the sheet, on the side where the latter transmits the tensile force. This rule was not defeated by any of the three parametric studies that were done. The cracking of the sheets with a priming on the internal face and then a propagation in the direction of the thickness of the sheet and then laterally in the sheet is therefore logical and supported by the calculations of the stresses, carried out on the internal side of the sheets.

The figure18, on the right, gives the same schematic representation as figure18 on the left but on the minimum diameter CD of the molten core. On this diameter, it is always the tangential stress σ_{23} which takes precedence over the normal stress σ_{33} , especially in the precise place where both reach their maximum values. This state of affairs has always been respected by each of the three parametric studies carried out. The ruin of the point welded by shear of the molten core, observed during the experiments mainly for high loading levels, is therefore plausible with regard to the distributions of the stresses obtained.

There is in fact a competition between the two modes of failure of the spot-welded specimen during tensile-shear fatigue tests. The respective stress concentrations on the internal face of the sheets and on the minimum diameter of the molten core simultaneously generate localized fatigue damage at the sites where the stresses are maximal. figure19 describes the location of the sites of initiation and cracking of the specimen welded by point and subjected to tensile-shear.

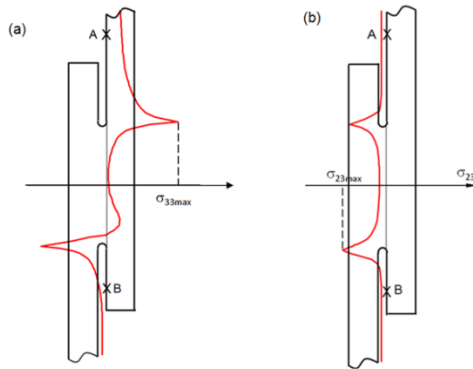


Figure 18.1 Distribution of the stresses (a) normal and (b) tangential along the segment AB

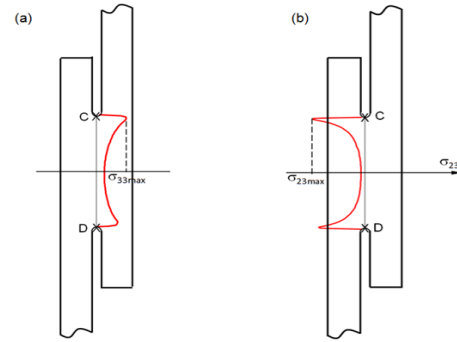


Figure 18.2 Distribution of the stresses (a) normal and (b) tangential along the diameter CD

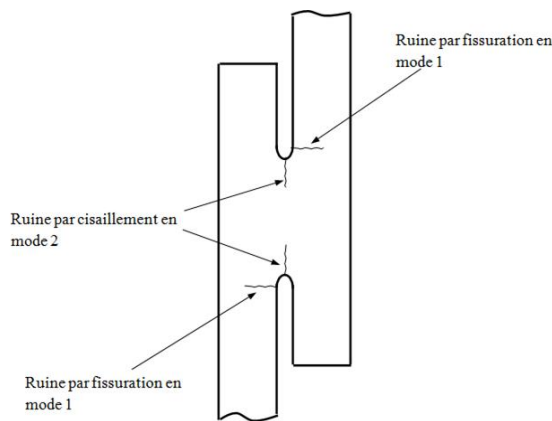


Figure 19 Experimental sites for the initiation and cracking of the test piece

3.4. Plate bending and stiffener influence

The behavior of the specimen under tensile-shear loading reveals a more or less pronounced flexing of the sheets, depending on the thickness of the assembled sheets and the level of the traction load applied to the test piece. This bending is linked, on the one hand, to the displacement of the resultant of the force applied by the jaws of the machine to the assembly constituted by the sheet metal and the wedge with the average line of the sheet through which the force of On the other hand, to the distance between the sheets detected after welding.

The stresses existing in the upper sheet between the jaws of the machine and the welded point are the superposition of those related to the tensile force and those of the moment of flexion. The tensile stress due to the tensile force and the tensile stress also generated by the bending moment are added to the inner face of the upper sheet. The same tensile stress and the compression stress due to the bending moment are added to the tensile face. Figure20 gives a representation of the distribution of the normal stress σ_{33} on the two inner and outer faces of the upper sheet.

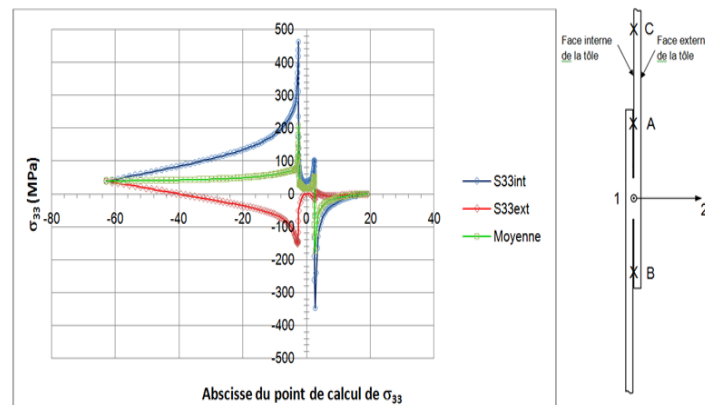


Figure20 Longitudinal distribution of the stress σ_{33} on the internal faces of C to D and external of the sheet

The stresses existing on one and the other of the two faces of the sheet are very different as the shape of the deformed of figure3.8a could allow it to be foreseen. The area of the welded point is of course the one of the highest stress concentrations. In order to ensure a pure shear-to-shear stress, in particular for specimens of small thickness, a stiffener is mounted and remains on each test piece tested during the test in order to limit the bending of the sheets and consequently too great a rotation of the Point welded around the axis 1 of the overall reference mark (figures. 4 and 8a). The resulting sheet peeling is added to the overall shear of the welded spot and is very unfavorable in terms of the experimental life of the specimen in the absence of a stiffener. In order to measure qualitatively the influence of the presence of the stiffener on the states of stress of which the sheets and the molten core are the seat, the calculations were carried out for three distinct cases:

- Test piece without stiffener,
- Test piece fitted with a stiffener with a lateral clearance of 0.2 mm,
- Test piece without play.

The modeling of the new boundary conditions generated by the stiffener is performed by means of the virtual contact pieces preventing the movement of certain zones of the test piece in the direction 2 of the global reference mark.

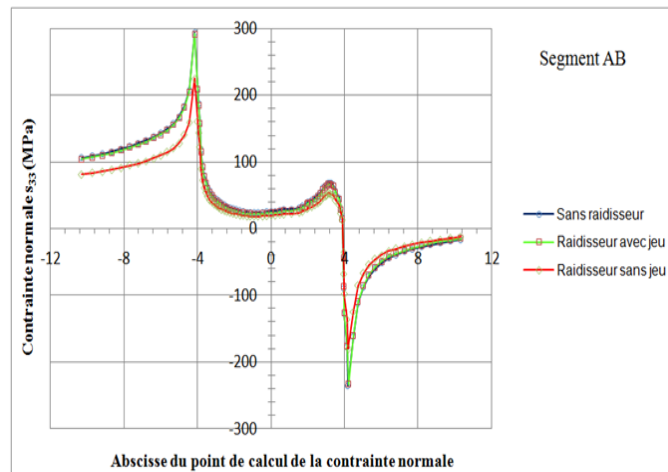


Figure 21 Distribution of the normal stress σ_{33} as a function of the presence or not of a stiffener and the lateral clearance test piece-stiffener

In figure 21, the distributions of the normal stress σ_{33} obtained in each of the three calculation cases on the inner face of the upper sheet were superimposed. The analysis of the results obtained unambiguously confirms the experimental observations made during the tests. There is practically no difference in stress peaks for the test specimen without stiffener and for which a stiffener with a clearance has been modeled. The possibility of moving in the interval corresponding to the existing clearance in direction 2 is sufficient to generate a behavior analogous to that corresponding to the absence of stiffener.

On the other hand, the presence of a stiffener without clearance induces a reduction in the peaks of stress observed at the foot of the fillet of connection of the molten core on the internal face of the sheet. This evolution of the stresses corroborates the experimental effect observed of the presence of a stiffener without play, namely an increase in the service life, ie a better fatigue strength of the welded point. The absence of stiffening-test piece clearance makes it possible to maintain a pure shear stress of the welded point, whereas in its absence the stress becomes rapidly mixed (shearing-peeling), which is more damaging in this case.

Recall that the problem of bending the sheets and pivoting the welded point about the axis 1 is essentially linked to the relatively small width of the test pieces. In practice, and for the same type of tensile-shear stress, the transverse part of the mechanical component provides rigidity such that the rotation of the welded point about the axis 1 is made very difficult or even is simply prevented. The particular geometry of the spot welded specimens does not have this transverse stiffness. The stiffener has appeared as a palliative to reproduce the maintenance in their plane of each sheet, in particular in the vicinity of the welded point.

4. STRESS ANALYSIS IN THE CASE OF THE ELASTOPLASTIC BEHAVIOR OF THE MATERIAL

The high concentration of the stresses existing in the welded spot and in its immediate vicinity may cause local lamination in some cases of heavy loading, such as during the application of the overloads. The objective of this section is to establish the distribution of the stresses from a modeling of the elastoplastic behavior of the steel

used to obtain a more realistic description of the real stresses in the most stressed zones, especially during the application Overloads. For this, a kinematic hardening was chosen. The stress distribution for elastoplastic behavior was calculated for two loading levels: 6000 N and 10 000 N. The distribution of the stresses calculated with a purely elastic behavior is superimposed on that of the elastoplastic behavior in order to Measure the relative difference between the results of the Finite Element calculations.

a) Load defined by a tensile force of 6000 N

The figures. 21 and 22 show the distributions of the normal stresses σ_{33} and tangential stress σ_{23} on the segment AB and on the diameter CD. There is essentially a relative decrease in the stress peaks observed on the minimum diameter of the melting point near the bottom of the notch and at the fillet of the molten core on the assembled sheets. There is no change in the location of these stress peaks. The presumed seed sites therefore remain identical in the two cases of behavior used. It is above all this point that appears to be the essential result, since it allows an elastic calculation, much faster in terms of calculation time, to locate the critical zones of the spot welded specimen.

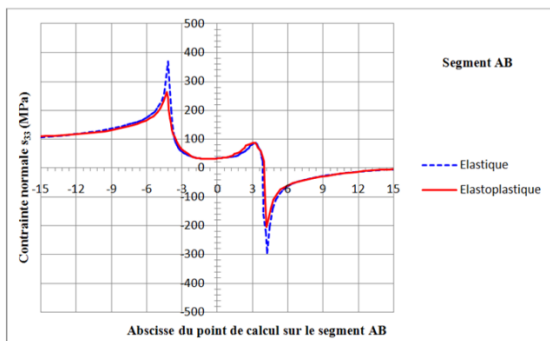


Figure 22.1 Distribution of the normal stress σ_{33} on the segment AB according to elastic or elastoplastic behavior of the material (for a tensile force of 6000 N)

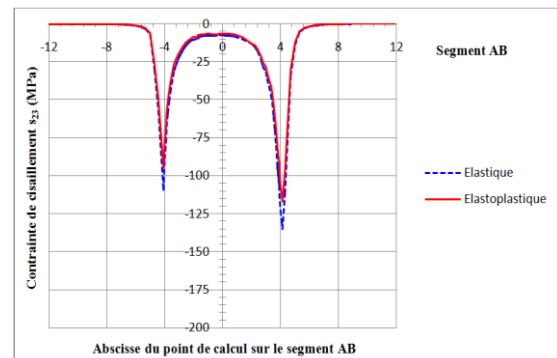


Figure 22.2 Distribution of the tangential stress σ_{23} on the segment AB according to elastic or elastoplastic behavior of the material (for a tensile force of 6000 N)

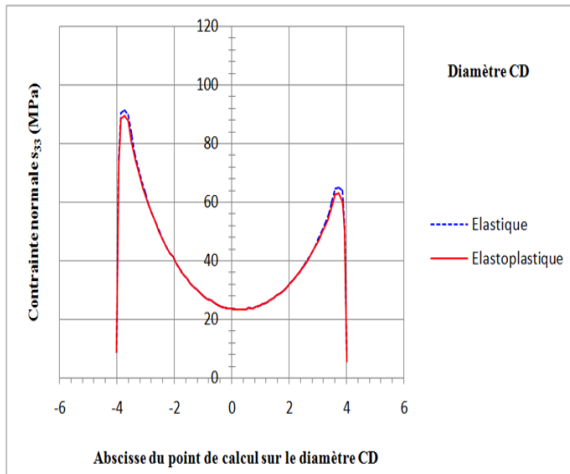


Figure 23.1 Distribution of the normal stress σ_{33} on the CD diameter according to elastic or elastoplastic behavior of the material (for a tensile stress of 6000 N)

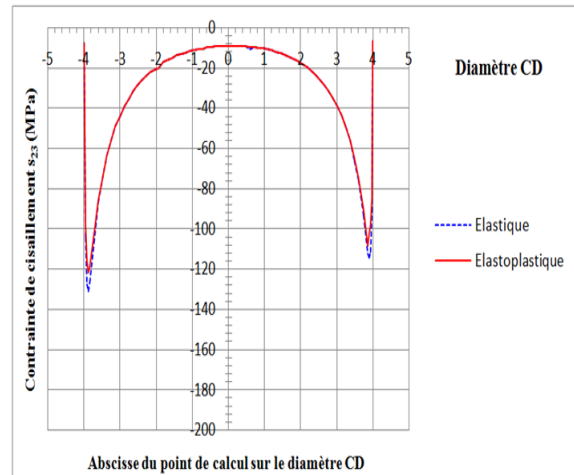


Figure 23.2 Distribution of the tangential stress σ_{23} on the CD diameter according to elastic or elastoplastic behavior of the material (for a tensile stress of 6000 N)

b) Load defined by a tensile force of 10 000 N

The figure24 gives the representation of the normal stress σ_{33} on the segment AB for a traction load of the test piece of 10 000 N this time under the hypothesis of an elastic or elastoplastic behavior. The difference between the stress peaks obtained for each of the two behaviors is marked but the localization of the peaks remains unchanged, validating the conclusions about the good correlation between the cracking sites observed experimentally and the prediction of the priming sites of d 'After the computation results of the constraints.

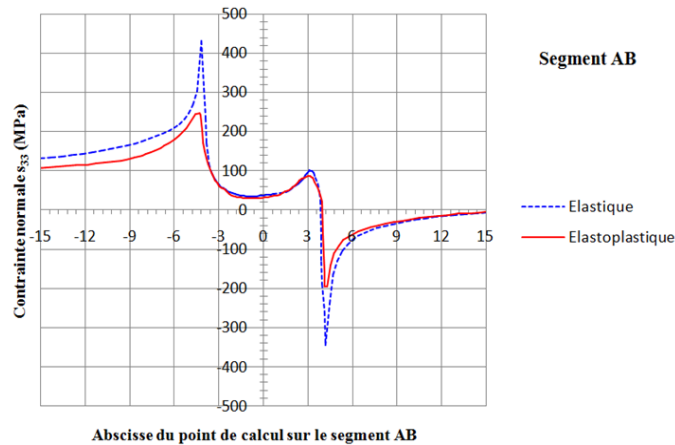


Figure 24 Distribution of the normal stress σ_{33} on the segment AB according to elastic or elastoplastic behavior of the material (for a tensile force of 10 000 N)

The time allowed for the calculation did not go beyond this analysis but it is very probable that one of the effects of the incidental overloads after the creation of a strong plastic deformation at the fillet of the molten core, Or the generation of residual compressive stresses in the same zone, which limits the character damage to "smaller" cycles between two overloads. The observed beneficial effect of overloads in the long life span is probably related to the creation of these residual stresses. The same is not true for the diameter CD, as regards the residual stresses, which explains the occurrence of the shear breaks of the points at lower loading levels of the base cycles when they are superimposed regularly overloads. In other words, the beneficial effect of the overloads is manifested on the segment AB and not on the CD segment probably by the creation of compressive residual stresses on the critical zone of AB which do not exist on the diameter CD.

5. CONCLUSION

The modeling and the calculation of a specimen welded by point and stressed in tension-shear made it possible to locate the critical zones or zones most stressed of the test piece. On the one hand, the sheet transmits the tensile force at the fillet of the molten core from the point welded to the sheet and on the other hand very close to the notch bottom in the molten core on the diameter parallel to the direction of the tensile force. Each of these two zones is stressed by multiaxial stress states which correspond mainly to tensile shear but of different nature: for the first zone, the tensile stress is preponderant very largely whereas for the second zone it is the stress of shear which is preponderant. From this point of view, the established model and the results of the calculations performed correlate very satisfactorily the experimental results obtained on the spot welded specimens. A parametric study was carried out on several geometric parameters which usually show certain dispersion for a batch of specimens made with a particular adjustment of the welding parameters. The diameter of the welded spot, the average distance between the two assembled plates and the shape of the notch bottom by the radius of the fillet of the molten core on the sheets are the three elements whose sensitivity of the dispersion on the calculation of the stresses was evaluated numerically. In all cases, a very clear sensitivity was observed on the maximum stress levels existing in the critical zones of the specimens. Qualitatively, the study carried out justifies the observed dispersion of experimental lifetime results even if the metallurgical hazards contribute equally and equally to these dispersions. In fact, it should be noted that the zones which are most mechanically stressed are also zones that are highly affected by heat, and therefore the site of strong phase and microstructure transformations. It would be interesting to relate the nature and stress levels established in the critical areas of the specimens to the fatigue life of these specimens. In addition to the role of the stress gradient, which is extremely important in critical areas, a second element complicates the implementation of a constraint approach for estimating lifetime; It is the characterization of the fatigue behavior of the new microstructures existing in the most stressed zones, very different from those of the base metal of which the plates are made. In the next chapter, a lifetime prediction approach is presented, the aim of which is to integrate the variable amplitude character of the load comprising the overloads with respect to that obtained at constant amplitude.

6. ACKNOWLEDGMENT

This work is the result of research carried out in the laboratory of Institute Pascal, University Blaise Pascal of Clermont-Ferrand (France)

I would like to thank Jean-Louis ROBERT, Nadjitonon NGARMAIM, Djonglibet WEL-DORET and N. KIMTANGAR for their participation in the production of this document.

Address:

- University Polytechnic of Mongo (Chad)
- BP: 4377/NDJAMENA

REFERENCES

- [1] ADIB H., JEONG J., PLUVINAGE G. *The three-dimensional finite element analysis of tensile-shear spot-welded joints in tensile and compressive loading conditions*. Strength of Materials, 2004, vol. 36. N°4, p. 353-364.
- [2] DANCETTE S. *Comportement mécanique des soudures par points : mécanismes et stratégies de prédiction dans le cas des tôles en acier pour automobile*, Thèse de l'INSA LYON, 2009, N° d'ordre 2009 – ISAL – 0039.
- [3] RADAJ D. SONSINO C. M., *Fatigue assessment of welded joints by local approaches*, Abington Publishing, 1998.
- [4] ROSSILLON F. *Influence des conditions de soudage sur le comportement en fatigue d'un acier THR Dual Phase soudé par point*. Thèse de l'Université Blaise Pascal – Clermont II, Clermont-Ferrand, Clermont-Ferrand, 2007.